

# Numerical Evaluation on Heat Transport Characteristics Between $\text{Al}_2\text{O}_3$ and ZnO Materials in Nanoscale Situation

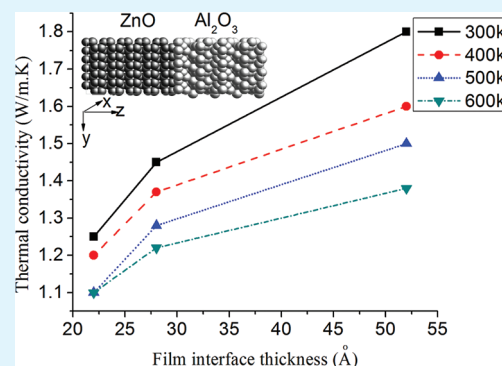
Ping Yang,<sup>\*,†</sup> Haifeng Xu,<sup>†</sup> Liqiang Zhang,<sup>†</sup> Fangwei Xie,<sup>†</sup> and Jianming Yang<sup>‡</sup>

<sup>†</sup>Laboratory of Advanced Design, Manufacturing & Reliability for MEMS/NEMS/ODES, Jiangsu University, Zhenjiang 212013, P. R. China

<sup>‡</sup>Faculty of Engineering and Applied Science, Memorial University, St. John's, NL A1B 3X5, Canada

**ABSTRACT:** The aim of this article is to provide a systematic method to perform numerical evaluation on the cross-plane thermal conductivity of  $\text{Al}_2\text{O}_3/\text{ZnO}$  film interface. The Equilibrium Molecular Dynamics (EMD) simulations method is used to investigate the cross-plane thermal conductivity of  $\text{Al}_2\text{O}_3/\text{ZnO}$  film interface along the direction of Z axis at different equilibrium temperature and film interface thickness. The Buckingham two-body potential function and Green–Kubo linear response theory are used for modeling and calculation. The results show that the size effect is obvious. It implies the film interface thickness is 23.4–52 Å and the equilibrium temperature is 300–600 K. The cross section thermal conductivity of  $\text{Al}_2\text{O}_3/\text{ZnO}$  film interface increases with the increase of interface thickness, and decreases with the increase in equilibrium temperature.

**KEYWORDS:** molecular dynamics simulations,  $\text{Al}_2\text{O}_3/\text{ZnO}$  film interface, Buckingham potential function, thermal conductivity



## 1. INTRODUCTION

The understanding of interface between oxide materials may develop a generation of new devices manufacturing. With the development of microelectronics technology, the nanoscale influence of thermal conduction between the interface structures becomes more and more serious in microelectronic devices. In the recent years, driven by the ongoing trend of miniaturization and function integration, thermal, mechanical and thermo-mechanical design, reliability and qualification of microelectronic device manufacturing are drawing more attentions from both industries and academic communities. With the logical devices in integrated circuit unit approaching nanodimension, the behaviors and properties of the micro/nano structures in the device are going to play a key role in the device performance. Therefore, the knowledge for the structure, cohesion and properties of the interfaces between metal/semiconductor, semiconductor/semiconductor or semiconductor/insulator in these devices becomes essential to the design and fabrication of them.<sup>1–18</sup>

Films are the common materials used in micro/nanoelectronic devices, and the micro/nanoelectronic devices' reliability and service life are directly affected by the heat conductive characteristics of the film.<sup>1</sup> The thermal conductivity of film was investigated by many researchers, for the nanofilm, the experimental method has many deficiencies, whereas the molecular dynamics (MD) simulations method is an effective manner. Lukes et al.<sup>2</sup> studied the thermal conductivity of solid thin-film by using the MD simulations, and the results showed that the thermal conductivity increase with the increase of the film thickness, as expected from thin-film experimental data and theoretical predictions; and this work showed that molecular

dynamics, applied under the correct conditions, is a viable tool for calculating the thermal conductivity of solid thin films. For multilayer film composed of different materials, interface is an important part, which affected the structural stability and heat conductive characteristics of the film. Xin-gang Liang<sup>3</sup> investigated the thermal resistance across doubled-layered nanofilm by using the nonequilibrium molecular dynamics (NEMD) simulations, and found that the thermal resistance was influenced by the interface structure, and the thermal conductivity of film was obviously affected by the interface effect. Yun-fei Chen<sup>4</sup> studied the thermal conductivity of Kr/Ar superlattice nanowires via NEMD method, and found that the effects of interface scattering and elastic strain were obvious. Volz<sup>5</sup> studied the heat transfer in Si/Ge superlattice using the MD techniques, and the effect of interface was discussed in detail. Ping Yang et al.<sup>6</sup> investigated the thermal behavior of the interface structure between two kinds of materials in micro/nano manufacturing by multiscale modeling and numerical analysis methods, and the results showed that the temperature distribution was nonuniform along the interface, and the main reason is the existence of the stress near the interface, which is caused by dissimilarity of material. The research of Abramson<sup>7</sup> indicated that for simple nanoscale strained heterostructures containing a single interface, the effective thermal conductivity might be less than half the average value of the thermal conductivities of the respective unstrained thin films, and the results showed that the thermal conductivity of thin

Received: September 3, 2011

Accepted: November 16, 2011

Published: December 14, 2011

film is greatly influenced by the interface. Hegedus<sup>8</sup> investigated the influence of interface on the thermal conductivity of heterogeneous system by using NEMD method. In this paper, NEMD software was developed to study thermal transport at the nanoscale. Results showed that the introduction of a second material into an argon film generally decreased its overall thermal conductivity. Moreover, the presence of a nanoparticle is less influential in reducing thermal conductivity than the addition of a thin layer. Stevens<sup>9</sup> studied thermal transport across solid–solid interface by using NEMD simulations, and found that the interfacial conductance decreases with the increase in mismatch, and there is a significant interfacial thermal transport dependence on temperature.

So far, the researches on interface heat conduction are mainly about metal–metal and metal–ceramic, whereas the heat conductive characteristics of ceramic–ceramic interface are rarely studied. Al<sub>2</sub>O<sub>3</sub> and ZnO are widely used in the optoelectronic devices. However, the thermal characteristics of Al<sub>2</sub>O<sub>3</sub> film and ZnO film, especially the Al<sub>2</sub>O<sub>3</sub>/ZnO film interface are rarely reported. To understand the thermal physical properties of Al<sub>2</sub>O<sub>3</sub> and ZnO, the thermal conductivity of Al<sub>2</sub>O<sub>3</sub>/ZnO film interface with different thickness and temperature is investigated by using MD simulations method. The results show the thermal conductivity with size effect and temperature effect, which can provide theoretical support for the design of the Al<sub>2</sub>O<sub>3</sub>/ZnO film interface structure in micro/nano manufacturing.

## 2. SIMULATIONS AND ANALYSIS

**2.1. Principle of MD Simulations.** In general, microscopic particles (molecules or atoms) are considered in MD simulations method.<sup>10</sup> Then the potential function is selected to describe the interaction force among particles in the MD system. The particles system is built by using Newton motion equation. The position and velocity of each particle at every moment can be obtained by solving the motion equations. The characteristics of the system are investigated by analyzing the motion state of particles. There are two basic assumptions for the MD simulation: (1) the motion of every particle follows the classic Newton's laws; (2) the interaction between particles adapt to superposition principle. Therefore, the MD simulation is a kind of approximate calculation model, which ignores the quantum effect. The Newton motion equation of particle can be shown as follows

$$\ddot{\mathbf{r}}_i = \mathbf{F}_i/m_i = \sum_{j \neq i} \mathbf{f}_{ij}/m_i \quad (1)$$

The force of atom  $i$  suffered can be obtained by

$$\mathbf{F}_i = -\partial U_i(r_1, r_2, \dots, r_n)/\partial \mathbf{r}_i \quad (2)$$

where,  $U(r_1, r_2, \dots, r_n) = \sum_{i=1}^n \sum_{j \neq i} \phi(r_{ij})$  is the total potential energy of the system;  $\phi(r_{ij})$  is the interatomic potential function between atom  $i$  and  $j$ .

The simulations are performed in the canonical ensemble (NVT), and Nose–Hoover heat bath method<sup>11</sup> is used to control the temperature of the system. The motion equation of the system can be described as follows

$$\dot{\mathbf{r}}_i = \mathbf{p}_i/m_i \quad (3)$$

$$\dot{\mathbf{p}} = \mathbf{F}_i - \xi(r_i, \mathbf{p}_i)\mathbf{p}_i \quad (4)$$

where,  $m_i$ ,  $r_i$ ,  $\mathbf{p}_i$  represent the mass, position, momentum of atom  $i$ , respectively.  $\xi$  is a coefficient, and it can be described as:

$$\xi = \sum_i (\mathbf{p}_i \cdot \mathbf{f}_i) / \sum_i |\mathbf{p}_i|^2 \quad (5)$$

**2.2. Computation of Thermal Conductivity.** The EMD method is used to calculate the thermal conductivity of Al<sub>2</sub>O<sub>3</sub>/ZnO film interface, and its theoretical basis of EMD method is the Green-Kubo linear response theory. In the scale of linear response, the Green-Kubo relation shows that the thermal conductivity can be obtained by the time correlation of the system's micro heat flux, which can be described as follows

$$k = \frac{V}{3k_B T^2} \int_0^\infty \langle J(t)J(0) \rangle dt \quad (6)$$

where  $k_B$  is the Boltzmann constant;  $T$  is the equilibrium temperature;  $J$  is the effective heat flux; and  $J$  can be described as

$$J = \frac{1}{V} \left[ \sum_i e_i v_i + \frac{1}{2} \sum_{i \neq j} r_{ij} (f_{ij} \cdot v_{ij}) \right] \quad (7)$$

where  $V$  is the system volume;  $v_i$  is the particle velocity;  $r_{ij}$  is the distance between the particle  $i$  and  $j$ ;  $r_{ij} = r_i - r_j$ ;  $f_{ij}$  is the force the particle  $j$  on particle  $i$ ;  $e_i$  is the total energy of every particle.

$$e_i = \frac{1}{2} m v_i^2 + \frac{1}{2} \sum \phi(r_{ij}) \quad (8)$$

**2.3. Modeling and Potential Function.** The simulating model of Al<sub>2</sub>O<sub>3</sub>/ZnO film interface is built. There are four types of crystal structure for ZnO. In this paper, the wurtzite structure is adopted for modeling because this crystal structure is similar with that of Al<sub>2</sub>O<sub>3</sub>. It implies that we can fabricate a more stable interface structure with two kinds of compatible crystal structures. The unit cell (UC) is taken as the unit, and the size of the model is controlled by the number of UC. The lattice parameters for ZnO were  $a = b = 0.325$  nm,  $c = 0.521$  nm,  $\alpha = \beta = 90^\circ$ ,  $\gamma = 120^\circ$ , the lattice parameters for Al<sub>2</sub>O<sub>3</sub> were  $a = b = 0.476$  nm,  $c = 1.3$  nm,  $\alpha = \beta = 90^\circ$ ,  $\gamma = 120^\circ$ . The model of Al<sub>2</sub>O<sub>3</sub>/ZnO film interface is shown in Figure 1.

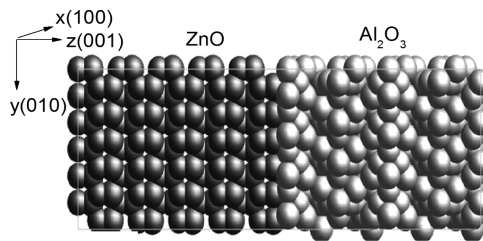


Figure 1. Model of Al<sub>2</sub>O<sub>3</sub>/ZnO film interface.

The interatomic potential function is requisite for calculating the equilibrium configuration of atoms by using the MD simulations method. The Buckingham potential function is used in our model by referencing literatures<sup>12–14</sup> and it can be given as follows

$$\phi(r_{ij}) = \frac{q_i q_j}{r_{ij}} + A \exp\left(\frac{-r_{ij}}{\rho}\right) - \frac{C}{r_{ij}^6} \quad (9)$$

where the first, second, and third terms corresponded to Coulomb repulsive, interaction, and van der Waals attraction energies, respectively;  $q$  is the effective charge of ions, which is assumed to be 60% of that of full charge;  $A$ ,  $\rho$ , and  $C$  are the coefficients shown in Table 1. The interaction at the interface can be obtained with the same method in ref 15.

**Table 1. Parameters of Buckingham Potential Function**

coefficients type	$A$ (eV)	$\rho$ (Å)	$C$ (eV Å)
O–Zn	529.70	0.3581	0.0
O–O	9547.9	0.2191	32.0
Zn–Zn	0.0	0.0	0.0

**2.4. Initial Conditions.** The initial conditions include simulating time, cutoff radius, and the size of cross-section, which affect the accuracy and the efficiency of the MD model. The periodic boundary conditions are set along the  $x$  direction and  $y$  direction of the model. Those initial conditions are discussed as following:

**2.4.1. Simulation Time.** Simulation time will affect the results of MD simulations. The simulation cannot approach to equilibrium if the simulation time is too short. To guarantee the calculation accuracy, as well as decrease the calculation time, the simulation time can be obtained by actual testing calculation. The time step is set as 1 fs according the manual of ME (Materials Explore) and ref Figure 2 shows the relationship

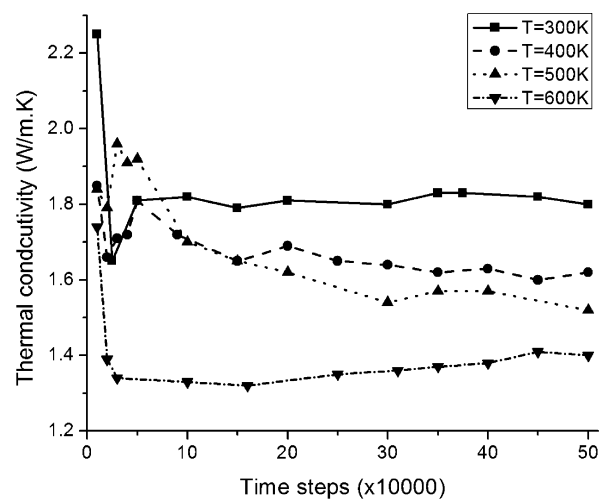


**Figure 2.** Relationship between the thermal conductivity and the time steps at different temperatures.

between the thermal conductivity and time steps at different temperatures (300, 400, 500, and 600 K). It indicates that the computation can approach to equilibrium when the time steps is 450 000 (simulation time is 0.45 ns) at different temperatures; and the thermal conductivity fluctuate slightly. Therefore, the simulation time is chosen as 0.5 ns (time steps is 500 000).

**2.4.2. Cut-off radius.** To improve the computational efficiency, the potential energy should be cut off in the actual simulation. The common method is spherical truncation method. The cutoff radius is important for simulation. In theory, the bigger the cutoff radius, the higher the calculating precision; however, the number of the interacting particles also increase, which make the calculating speed slower. Figure 3

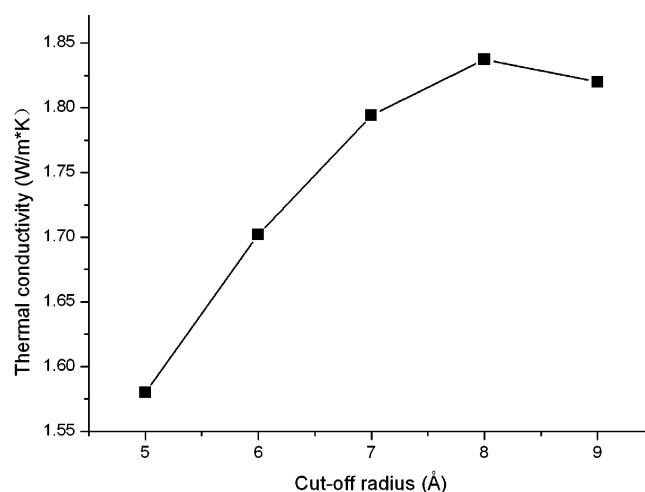


**Figure 3.** Relationship between the thermal conductivity and the cutoff radius.

shows the calculated results about thermal conductivities at different cutoff radius. It shows that the thermal conductivity falls between 1.8 and 1.85 W/m K when the cutoff radius increases from 7 to 9 Å, and there is no significant change, whereas the computation increases obviously. By considering the computational complexity and the simulation accuracy, the cutoff radius is chosen as 7 Å. Thus, the interaction among the particles outside the cutoff radius can be ignored.

**2.4.3. Cross-Section Dimension.** The thermal conductivity of  $\text{Al}_2\text{O}_3/\text{ZnO}$  film interface is calculated with the thickness of 52 Å. Figure 4 shows the relationship between the thermal

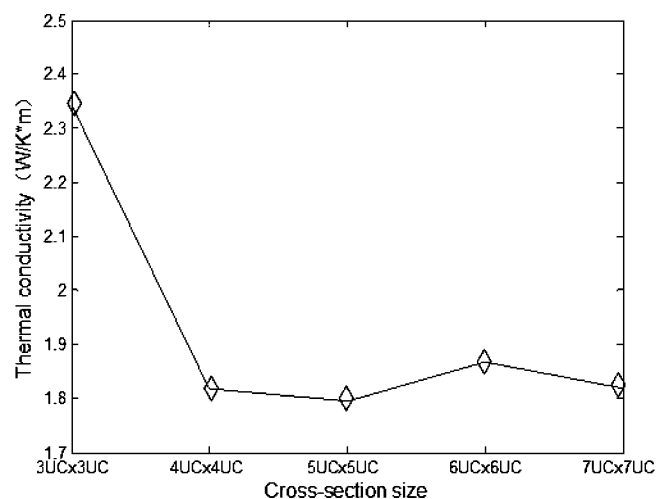


**Figure 4.** Relationship between the thermal conductivity and the cross-section dimension.

conductivity and the cross-section dimension. It indicates that the thermal conductivity changes inconspicuous with the increases of cross-section dimension, and the average thermal conductivity is about 1.8 W/m·K. Figure 5 shows the relationship between thermal conductivity and the time steps. With the increases of the time steps, the thermal conductivity becomes stable, and approach to a certain value. The change of the curves about 5UC × 5UC and 6UC × 6UC are relatively stable than that of 4UC × 4UC. The cross-section of 5UC × 5UC can fast converge to 1.8 W/m K. With the increase of

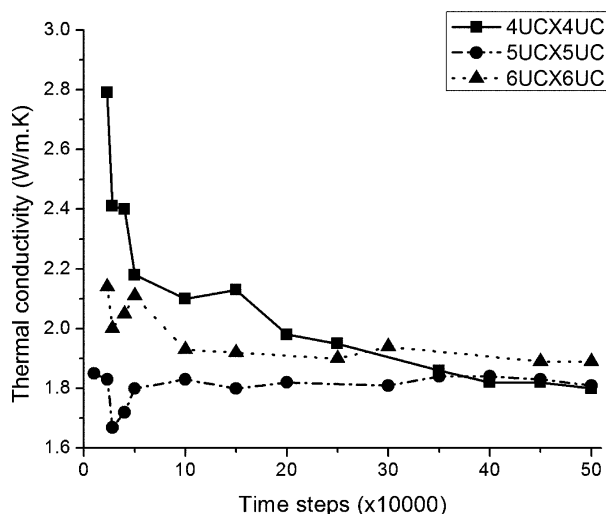


**Figure 5.** Relationship between thermal conductivity and the simulation time at different cross-section dimension.

cross-section dimension, the number of atoms increases, which cause the computation more complex. To ensure the calculation accuracy and minimizing the computational complexity, the cross-section dimension of  $SUC \times SUC$  is selected for simulation.

### 3. SIMULATION RESULTS

Figure 6 shows the relationship between the thermal conductivity and the interface thickness of ZnO and  $Al_2O_3$ . It

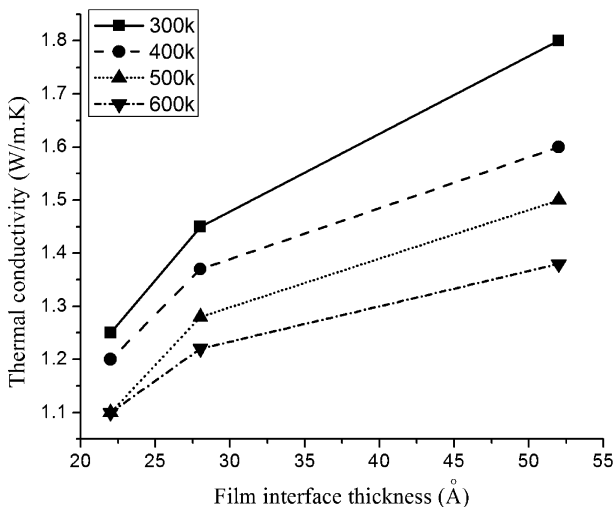


**Figure 6.** Relationship between the thermal conductivity and the interface thickness of ZnO and  $Al_2O_3$ .

indicates that the size effect is obvious, and the thermal conductivity of  $Al_2O_3/ZnO$  film interface increases with the increase of interface thickness (the error limits of each data is  $\pm 0.0218W/K \cdot m$ ). The possible reason is the boundary scattering change of the thermal carriers. For ceramics materials, phonon is the main thermal carrier, and the thermal energy is transmitted through phonon conduction. The mobility of the phonons determines the thermal transport properties of the film. Based on the kinetic theory,<sup>16</sup> the thermal conductivity can be written as  $K = Cvl/3$ , where  $l$  is the mean free path of the

dominant phonons,  $C$  is the phonon specific heat and  $v$  is the average speed of sound. Boundary scattering increases with the increase of the ratio ( $l/d$ ,  $d$  is the layer thickness).<sup>19</sup> It induces the value of thermal conductivity increase with the increase of interface thickness because the boundary scattering function approach to weak situation.

Figure 7 shows the relationship between the thermal conductivity and the temperature. It indicates that the thermal

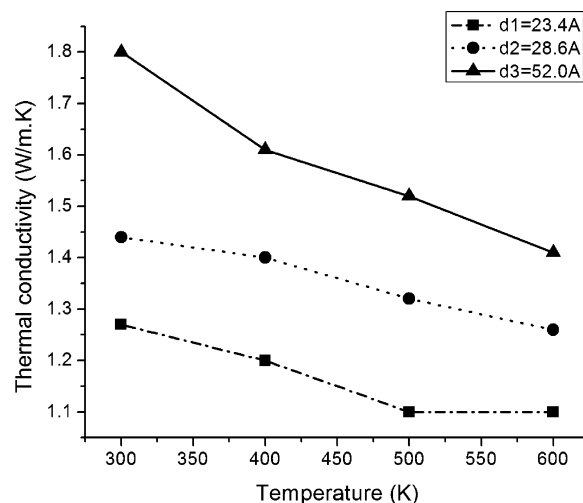


**Figure 7.** Relationship between the thermal conductivity and the temperature.

conductivity of  $Al_2O_3/ZnO$  film interface decreases with the increase of the temperature. The reasons can be induced as following: (1) with the increase of temperature, the phonon scattering function enhances and the mean free path of the dominant phonons decreases. (2) Because of the difference in structure and material property between  $Al_2O_3$  and ZnO, there will be some voids in the interface, which affects the heat conduction. Meanwhile, the existence of the interface thermal resistance also decreases the thermal conductivity.

### 4. CONCLUSIONS

The thermal conductivities of  $Al_2O_3/ZnO$  film interface with different thickness and temperature are calculated by using the EMD simulations. The interface thickness is from 2.34 nm to 5.2 nm, and the temperature is from 300 to 600 K. The simulation results show that the size effect and temperature effect are obvious. The thermal conductivity increases with the increase of interface thickness (23.4–52 Å). The thermal conductivity decreases with the increase of temperature, which caused by the enhancement of the phonon scattering and the decrease of the mean free path of the dominant phonons. So a systematic method is developed to perform numerical evaluation on the cross-plane thermal conductivity of  $Al_2O_3/ZnO$  film interface, which can build a theoretical basis for fabricating the  $Al_2O_3/ZnO$  film interface in micro/nano-manufacturing.

### ■ AUTHOR INFORMATION

#### Corresponding Author

\*E-mail: yangpingdm@ujs.edu.cn or yangping1964@163.com. Tel: +86-511-88790779.

## ■ ACKNOWLEDGMENTS

The authors acknowledge the support of National Natural Science Foundation of China (61076098), the Special Natural Science Foundation for Innovative Group of Jiangsu University and the support of Innovative Foundation for Doctoral candidate of Jiangsu Province (CX10B\_252Z) during the course of this work. Ph.D. candidate Liqiang Zhang is the co-first author of this paper.

## ■ REFERENCES

- (1) Chou, F. C.; Lukes, J. R.; Liang, X. G.; Tankahashi, K. *Annu. Rev. Heat Transfer* **1999**, *10*, 141–176.
- (2) Lukes, J. R.; Li, D. Y.; Liang, X. G.; Tien, C. L. *Trans. ASME, Ser. C* **2000**, *122*, 536–543.
- (3) Xin-gang, L.; Sun, L. *Microscale Thermophys. Eng.* **2005**, *9*, 295–304.
- (4) Yunfei, C.; Deyu, Li; Juekuan, Y. *Physica B* **2004**, *349*, 270–280.
- (5) Volz, S.; Saulnier, J. B.; Chen, G.; Beauchamp, P. *Microelectron. J.* **2000**, *31*, 815–819.
- (6) Yang, P.; Liao, N. B. *Appl. Phys. A: Mater. Sci. Process.* **2008**, *92*, 329–335.
- (7) Abramson, A. R.; Tien, C. L.; Majumdar, A. *J. Heat Transfer* **2002**, *124*, 963–970.
- (8) Hegedus, P. J.; Abramson, A. R. *Int. J. Heat Mass Transfer* **2006**, *49*, 4921–4931.
- (9) Stevens, R. J.; Zhigilei, L. V.; Norris, P. M. *Int. J. Heat Mass Transfer* **2007**, *50*, 3977–3989.
- (10) Rapaport, D. C. Cambridge University Press: New York, 1995; pp 1–3.
- (11) Allen, M. P.; Tildesley, D. J. *Computer Simulation of Liquids*; Oxford University Press: New York, 1989; p 230.
- (12) Gutierrez, G. *Phys. Rev. B* **2002**, *65*, 104202.
- (13) Adiga, S. P.; Zapol, P.; Curtiss, L. A. *J. Phys. Chem. C* **2007**, *111*, 7422–7429.
- (14) Kulkarni, A. J.; Zhou, M.; Ke, F. J. *Nanotechnology* **2005**, *16*, 2749–2756.
- (15) Dmitriev, S. V.; Yoshikawa, N.; Kohyama, M.; Tanaka, S.; Yang, R.; Kagawa, Y. *Acta Mater.* **2004**, *52*, 1959–1970.
- (16) Majumdar, A. *J. Heat Transfer* **1993**, *115*, 7–16.
- (17) Liao, N. B.; Yang, P.; Zhang, M.; Xue, W. *Mater. Sci. Eng., A* **2010**, *527*, 6076–6081.
- (18) Yang, P.; Wu, Y. S.; Xu, H. F.; Xu, X. X.; Zhang, L. Q.; Li, P. *Acta Phys. Sin.* **2011**, *60*, 066601.
- (19) Flik, M. I.; Choi, B. I.; Goodson, K. E. *J. Heat Transfer* **1992**, *114*, 666–674.